

Electromagnetic properties of natural expansive soils under one-dimensional deformation

Botao Lin · Amy B. Cerato

Received: 16 February 2012 / Accepted: 14 November 2012 / Published online: 4 January 2013
© Springer-Verlag Berlin Heidelberg 2013

Abstract Macroscopic behavior of expansive soil is governed by surface forces rather than gravitational forces. These physicochemical surface forces can be investigated through two electromagnetic properties in response to an applied electromagnetic field as real (relative) permittivity, κ' , and effective (electrical) conductivity, σ . This paper presents the results of dielectric measurements on four natural expansive soils using 1–100 MHz electromagnetic waves in two different test setups. The equipment setup, calibration process and measurement limitations are evaluated, and the dielectric spectra, in terms of the dispersion of real permittivity/effective conductivity with frequency, are presented. A procedure is presented to quantify the thickness of a fully developed diffuse double layer (DDL). The influence of salt concentration on DDL, as well as the dielectric responses, is assessed. Two parameters of special physical meaning are defined in the article: κ'_{inf} , representative of the dielectric response by sample mineralogy, microstructure and saturation ratio, and σ_{dc} , combining the roles assumed by both surface conduction and pore fluid conduction. Evaluation is attempted on their magnitudes at the optimum compaction state and evolutions at different one-dimensional deforming stages. Extensive analysis is performed on the roles of κ'_{inf} and σ_{dc} on the hydration status and structural anisotropy of an oedometer sample.

Keywords Diffuse double layer · Electromagnetic properties · Expansive soils · One-dimensional deformation · Surface conductance/conductivity

1 Introduction

Expansive soil experiences volumetric swelling or shrinkage with climatic fluctuations. The macroscopic behavior of expansive soil in terms of volume change and shear strength is governed by individual clay platelets that are mostly controlled by surface physicochemical forces, instead of gravitational forces, due to their small size and the diffuse double layer formed around clay platelets. Therefore, a comprehensive mechanical framework of expansive soil lies in understanding the surface phenomena determined by various physicochemical forces. This article is dedicated to the electromagnetic properties that can be used to explain microscopic mechanisms due to physicochemical forces.

Soil can be viewed as a dielectric with electromagnetic properties of magnetic permeability, real (relative) permittivity, κ' , and effective (electrical) conductivity, σ . Since most natural soils are non-ferromagnetic, the latter two (real permittivity and effective conductivity) are able to fully characterize the dielectric responses of soil to an electromagnetic field [1, 31]. In practice, these two properties have been used to monitor soil moisture [32], predict porosity [2] and determine the presence of contaminants [33] and sulfates [8]. It has also been shown that in clay minerals, κ' and σ vary as a function of frequency, the phenomenon of which is called dielectric dispersion or relaxation [4] as a result of certain polarization mechanisms, with the corresponding curves described as dielectric spectra [1]. The magnitude of dielectric dispersion in the radio frequency range (0.1 MHz–1 GHz) is defined as the difference in magnitude at high and low frequencies at which the real permittivity or effective conductivity curve levels off. This value has been shown to be a function of the mineralogy and mineral solution interface characteristics, for example, minerals of higher specific surface area usually exhibit higher dispersion

B. Lin · A. B. Cerato (✉)
School of Civil Engineering and Environmental Science,
University of Oklahoma, Norman, OK 73019, USA
e-mail: acerato@ou.edu

magnitudes than those of lower surface area [1]. Over the frequency range of 1 MHz–1 GHz, interfacial polarization has been identified as the predominant mechanism contributing to the dielectric dispersion behavior of fine-grained soils. Bound water polarization is negligible in the range of 1 MHz–100 MHz and only slightly affects the dielectric spectra at frequencies higher than 100 MHz [18]. Interfacial polarization occurs as charge accumulation at the interfaces between soil constituents in order to maintain the same current density across different constituents, while bound water polarization stems from directional alignment of adsorbed water on soil particle surfaces [31].

Most of the above research involves measurements using a two-terminal electrode system with a frequency range from several Hz to less than 100 MHz. For expansive soils, it is desirable to investigate electromagnetic properties during swelling or compression, for which the two-terminal electrode system is the most suitable option because the testing configuration is able to accommodate one-dimensional deformation of the test sample. Cerato and Lin [10] proposed one approach to measure electromagnetic properties of soil–electrolyte mixtures in a modified oedometer cell using electromagnetic waves with a frequency range from 400 kHz to 20 MHz. A major problem associated with this type of measurement lies in the phenomenon of electrode polarization, which originates from charge accumulation at the electrode–sample interface that artificially increases the measured real permittivity or decreases the obtained effective conductivity at low frequencies up to several MHz [7, 13, 26]. The measured effective conductivity is minimally affected by electrode polarization at kHz frequencies and higher, while the polarization can strongly affect the measurements of relative permittivity at the same frequencies [15, 31]. Additionally, as the salt concentration in the liquid phase increases, the frequency at which electrode polarization manifests in the measurement of real permittivity can increase significantly, while effective conductivity observations show negligible changes [7, 16]. Klein and Santamarina [14] introduced a four-terminal electrode system to avoid the effects of electrode polarization by using separate current injection and potential monitoring electrodes. However, the test setup involves inserting a pair of needle-shaped electrodes into the middle of the soil sample, which may create disturbance to the sample when deformed. This research is devoted to understanding the dielectric responses of four field-collected natural expansive soils under one-dimensional hydromechanical conditions.

Liu and Mitchell [18] developed a physically based model to predict dielectric spectra for sand, silt, pure clay and mixtures of sand and pure clay based on a series of predetermined and optimized physicochemical parameters.

The three optimized parameters include the direct current (dc) conductivity of pore fluid, surface conductance and shape factor. While the former two can be experimentally determined or approximated, the last one, which was taken as the average length ratio of the long over the short axis of individual particles, must be assumed or optimized. This parameter is especially complicated to determine in natural clayey soils because a variety of clay minerals coexist. Furthermore, the physicochemical interaction between clay and sand or silt or between various clay minerals was not taken into account in the model. The results of the dielectric spectra of expansive soils in this research provide a database for future validation and improvement of the model, especially on clayey soils.

2 Characterization of the studied soils

Four expansive soils were selected in this study with their common geotechnical properties listed in Table 1 (obtained following ASTM [6]).

Some physicochemical characteristics are listed in Table 2. The total specific surface area S_a was attained following the EGME surface area method [11]. The test involved saturating a soil sample with Ethylene Glycol Monoethyl Ether (EGME) and then removing the excess EGME in a vacuum desiccator until the EGME formed a monomolecular layer on the soil surface. The pH value was measured according to ASTM D4972 [6]. The cation exchange capacity (CEC) and percentages of exchangeable cations were determined by Harris Laboratory, Inc., Lincoln, Nebraska, using a 1 N ammonium acetate extraction method [30]. The surface conductance, λ_{ddl} , can be estimated as the product of surface charge density and cation mobility [31], which is written in the following form [17]:

$$\lambda_{ddl} = \frac{\sum u_i P_i \cdot \text{CEC}}{S_a} \quad (1)$$

where u_i is cation mobility; P_i is percentage of each cation (in quantity).

The much higher mobility of hydrogen ($36.2 \times 10^{-8} \text{ m}^2 \text{ V}^{-1} \text{ s}^{-1}$) than the other cations and the significant hydrogen concentration produce a large λ_{ddl} (7.97×10^{-8}) of Carnisaw, which falls sharply to a magnitude of 1.7×10^{-9} if excluding the effect of hydrogen. The validity of the contribution of hydrogen to λ_{ddl} will be challenged in the discussion later. Equation (1) also assumes that the anionic deficit in the diffuse double layer is zero, whereas in reality λ_{ddl} is dependent on both the concentration of excess cations and the deficit of anions, in which the latter is much smaller than the former and can be neglected in estimation [15]. A correction factor was introduced for

Table 1 Common geotechnical properties of the four studied soils

Test sample	w_{opt}^a (%)	ρ_{dmax}^a (Mg/m ³)	G_s (–)	S^b (%)	LL (%)	PL (%)	PI (%)	CF (%)	q_u^b (kPa)	Δh^b (%)	p_s^b (kPa)	ψ_m^b (kPa)	USCS
Carnisaw	26.2	1.62	2.8	98	59	32	27	51	578	2.3	75	469	MH
Hollywood	20.6	1.67	2.8	85	54	20	34	62	365	5.6	141	758	CH
Heiden	24.2	1.55	2.8	84	67	23	44	50	313	9.3	230	1120	CH
Eagle Ford	27.1	1.42	2.7	81	92	35	57	66	304	12.7	263	1126	CH

w_{opt} optimum moisture content, ρ_{dmax} maximum dry density, G_s specific gravity, S degree of saturation, PI plasticity index, CF clay size fraction, q_u unconfined compressive strength, Δh swell potential (seating load = 1 kPa), p_s swell pressure, ψ_m matric suction (pressure plate test), *USCS* unified soil classification system

^a Standard proctor test

^b At or from the optimum state (w_{opt} and ρ_{dmax})

Table 2 Some physicochemical characteristics of the studied soils

Test sample	pH	S_a (m ² /g)	CEC (meq/100 g)	K (%)	Mg (%)	Ca (%)	Na (%)	H (%)	λ_{ddl} ($\times 10^{-8}$ S)
Carnisaw	4.4	108	27.3	0.9	9.1	1.8	0.2	88	7.97 ^a /0.17 ^b
Hollywood	7.2	146	26.4	1.3	4.6	93.2	1.0	0	1.08
Heiden	8.7	229	50.7	0.8	11.0	82.2	6.0	0	1.30
Eagle Ford	7.7	214	49.6	1.5	13.2	77.8	7.5	0	1.36

S_a specific surface area (total), *CEC* cation exchange capacity, λ_{ddl} estimated surface conductance, *Na* sodium, *Ca* calcium, *Mg* magnesium, *K* potassium

^a Taking into account the contribution of hydrogen

^b Excluding the effect of hydrogen

Table 3 Summary of the geological and geotechnical descriptions

Test sample	Geological classification	Geotechnical description	Clay size minerals (%) ^a
Carnisaw	Residuum weathered from shale of Pennsylvanian age	Red brown silty clay or elastic silt	V (12), I (25), KA (14)
Hollywood	Clayey colluvial sediments over limestone of Cretaceous age	Yellowish olive fat clay with trace of light gray limestone	M (23), I (21), KA (18)
Heiden	Clayey shale of Cretaceous age	Olive gray highly plastic fat clay with trace of organic root	M (37), I (5), KA (8)
Eagle Ford	Fossiliferous clayey shale with sandy shale lenses	Yellowish tan highly plastic pure clay	M (28), I (27), KA (11)

^a *V* vermiculite, *M* montmorillonite, *KA* kaolinite, *I* illite; percentages were deduced following USGS [34] and multiplied by *CF* to represent the mineral proportion in the entire sample

justifying this deficit for a single chemical solute [15, 20], which was derived as a monotonical function of zeta potential on the basis of theoretical models of electrokinetic phenomena. In the soil cases of this study, such modeling efforts can be challenging in respect of the complex solutes in the bulk fluid. Moreover, the ionic mobility of the cations in the double layer was assumed to be the same as in a diluted solution, which in fact is prone to be restrained by a negatively charged surface.

The mineralogy of the soil samples was investigated through X-ray diffraction analysis. The results are jointly provided in Table 3 with other geological and geotechnical descriptions.

3 Electromagnetic test setup and procedure

The expressions for real (relative) permittivity and effective (electrical) conductivity are

$$\kappa' = \frac{\text{Im}(1/Z)}{\omega \epsilon_0 \alpha A/d} \quad (2)$$

$$\sigma = \frac{\text{Re}(1/Z)}{\beta A/d} \quad (3)$$

where $\epsilon_0 = 8.85 \times 10^{-12}$ F/m is the permittivity of vacuum; ω is the circular frequency; Z is the impedance of the sample; A is the area of each electrode and d is the spacing

between the two electrodes; α and β are the calibration factors for a specific electrode pair [10].

A HP 4193A vector impedance meter with 400 kHz–110 MHz frequency range powered the two-terminal electrode system. Open circuit, short circuit and standard circuit measurements were performed for the initial calibration of the equivalent circuit according to the HP 4193A operation manual. The calibration factors α and β were introduced by Cerato and Lin [10] for a given pair of electrodes. Usually, a calibration needs to be performed by testing a standard liquid or electrolyte with a constant value of κ' or σ (invariant within the radio frequency range) in order to obtain the actual values of κ' and σ of the sample under test. In the interest of measuring electromagnetic properties during soil deformation, the electrode spacing, d , should be able to change during the test. The ratio A/d is variable, therefore, and calibration factors should then be deduced with dependence on the electrode size and spacing. Parallel electrode pairs of various size and spacing were used to determine calibration factors with a detailed process discussed in Cerato and Lin [10]. The relationships between α and β and R_{eq}/d ($R_{eq} = \sqrt{A/\pi}$) were found to follow trends described by the following two equations:

$$\alpha = k_1 + m_1(R_{eq}/d)^{-n_1} \quad (4)$$

$$\beta = k_2 + m_2(R_{eq}/d)^{-n_2} \quad (5)$$

in which k_i , m_i and n_i ($i = 1, 2$) change with frequency. Their values were attained corresponding to each of the 43 sweeping frequencies (ranging from 400 kHz to 110 MHz) of the HP4193A in the automatic sweep mode. The R^2 value varies between 0.92 and 0.99 for the frequencies applied. As a result, the factors α and β not only change with R_{eq}/d but also vary with frequency. It must be noted that R_{eq}/d is used instead of A/d so that both sides of Eqs. (4) and (5) are dimensionless.

The two-terminal electrode system used in this study includes two setups for which the calibration was performed within a Faraday cage(s). The dielectric measurement normal to the direction of sample compaction (described as horizontal) was undertaken in the first setup (Fig. 1). In all the sample preparation and testing procedures, the ambient temperature was maintained to be 25.0 ± 0.5 °C. Each soil sample was initially compacted in a Plexiglas ring with a pair of slightly curved electrodes embedded in the inner wall. In this case, the calibration factors α and β only evolve with frequency because the electrodes shown in Fig. 1 are integrated in the ring so that the R_{eq}/d value is a constant. The ring was placed on a flat Plexiglas plate, and each sample was compacted in five layers to w_{opt} and γ_{dmax} (Table 1), using volume-based compaction. It is worth noting that each sample must be compacted directly inside the ring in order to ensure a

decent contact with the lateral electrodes. After compaction, the sample in the ring was sealed for moisture equalization in a humidity room for 2 weeks. During the test in the first setup (Fig. 1), the top and bottom surfaces of the sample were covered by cling wrap and Plexiglas plates to prevent loss of moisture. The copper wires were connected from the electrodes to the component adapter while both the ring and the adapter were enclosed in a Faraday cage. The reason for using a Faraday cage for both the calibration and test processes will be discussed later.

After the horizontal dielectric measurement was completed with the setup shown in Fig. 1, the soil sample was uncovered and carefully extruded with a hydraulic jack into another Plexiglas ring of the same size and dimension but with no electrodes and wires attached. The second ring was then installed in a modified oedometer cell as shown in Fig. 2, with the bottom and top stones containing flat electrodes for the dielectric measurement in the direction of compaction (marked as vertical). In Fig. 2, the value of R_{eq}/d varies with soil deformation. Therefore, the magnitudes of α and β vary with both frequency and R_{eq}/d in this setup and should be calculated from Eqs. (4) and (5) according to each test frequency. An initial seating load of 1 kPa was applied on the sample, and the measurement was taken. Afterward, de-ionized water was introduced to inundate the sample to let it experience free swelling under the seating load, and then the applied load was varied so that the sample underwent a series of stages including consolidation to the original height, rebounding under the seating load (1 kPa), and recompression to the initial height. Dielectric measurements were performed at the end of each swelling/compression stage.

Initially, it was thought that the dielectric measurements could be taken in both directions at the same time (i.e., the curved electrode pair embedded in the ring wall and the pair of flat electrodes in the bottom and top stones implemented simultaneously for both horizontal and vertical measurements), as was illustrated in the work of Cerato and Lin [10]. However, it was found that the two pairs of electrodes created interference with each other, as will be presented later. Therefore, the use of each pair must be isolated. In order to gather both horizontal and vertical measurements on an identical sample, the sample had to be extruded from the ring with the embedded curved electrodes into one without embedded electrodes after finishing the horizontal measurement. The sequence of first using the setup in Fig. 1 and then the setup shown in Fig. 2 cannot be reversed. Extruding the sample into the ring with the embedded curved lateral electrodes cannot assure a decent contact between the sample and the lateral electrode and may cause contamination of the lateral pair of electrodes with lubricant grease, which is commonly applied to minimize the soil–ring friction.

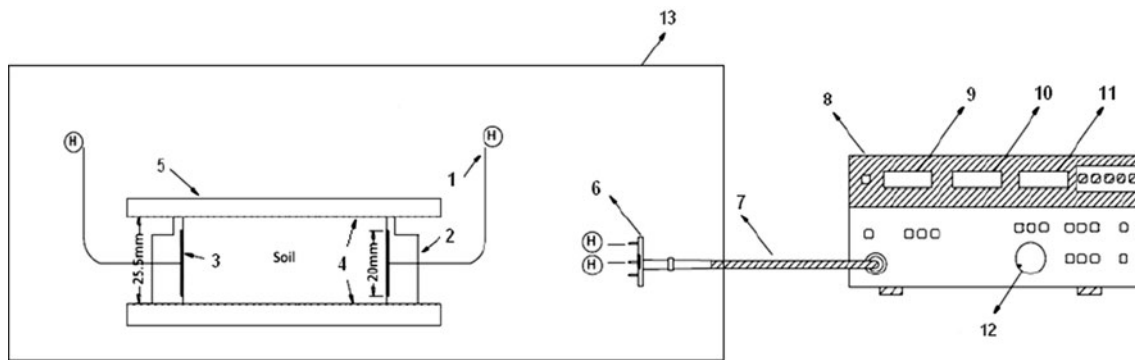


Fig. 1 Dielectric measurement setup 1: *H*—horizontal measurement (1 coated copper wire, 2 Plexiglas ring, 3 copper electrode, 4 cling wrap sheet, 5 Plexiglas plate, 6 component adapter, 7 probe, 8 HP 4193A vector impedance meter, 9 magnitude of impedance, 10 phase angle, 11 frequency, 12 frequency control dial, 13 Faraday cage)

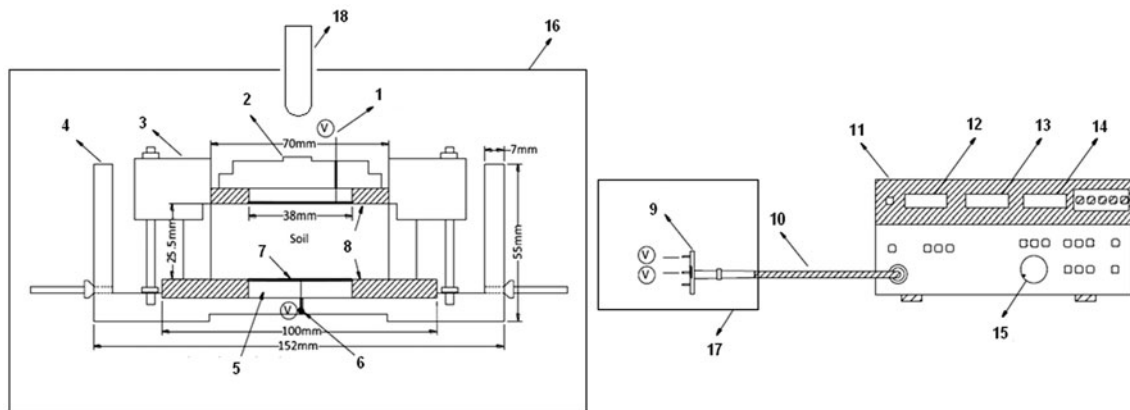


Fig. 2 Dielectric measurement setup 2: *V*—vertical measurement (1 coated copper wire, 2 Plexiglas cap, 3 Plexiglas frame, 4 Plexiglas cell, 5 indented Plexiglas plate, 6 notch for outreach of the bottom copper wire, 7 copper electrode, 8 porous stone, 9 component adapter, 10 probe, 11 HP 4193A vector impedance meter, 12 magnitude of impedance, 13 phase angle, 14 frequency, 15 frequency control dial, 16 Faraday cage 1, 17 Faraday cage 2, 18 loading piston)

4 Issues associated with the test method

4.1 Enclosure of the DUT using a Faraday cage

A Faraday cage is recommended to enclose the device under test (DUT) in order to block out potential external electromagnetic interference. It is practically an ideal hollow conductor which is able to rearrange charges produced by any externally applied electric fields leading to the cancellation of the applied field inside so that the internal atmosphere becomes neutral. The Faraday cages used in this research were made of copper mesh with a maximum opening of 6 mm, which is much less than the wavelengths of radio radiation of this study ($\approx 5\text{--}500$ m).

In order to evaluate the impact of a Faraday cage on the test results, horizontal measurements (with the setup shown in Fig. 1) were undertaken on Carnisaw and Eagle Ford samples with and without using a Faraday cage and the comparisons are presented in Fig. 3. In addition, a Minco

silt ($LL = 20$, $PI = 4$) sample of 15 % moisture content and 1.96 Mg/m^3 wet density was tested for its real permittivity curves for comparison with the findings of Varghese [35], which tested an identical compacted sample within a Faraday cage (Fig. 3). It must be noted that Varghese [35] failed to report effective conductivity data that would otherwise be useful for comparison with the effective conductivity data of this study.

The Faraday cage is insignificant in affecting real permittivity within the concerned frequency range (1 MHz–100 MHz), except at 40 MHz where a peak takes place because of electronic resonance. In terms of effective conductivity, σ , the most significance of the Faraday cage was again seen at the peaks around 40 MHz. Beyond this frequency, the external electrical interference results in slight deviation with respect to the measured effective conductivity. The close correspondence between the test data with and without Faraday cage implies that the test environment in this research (a basement room) had little external electromagnetic interferences. Nevertheless, to

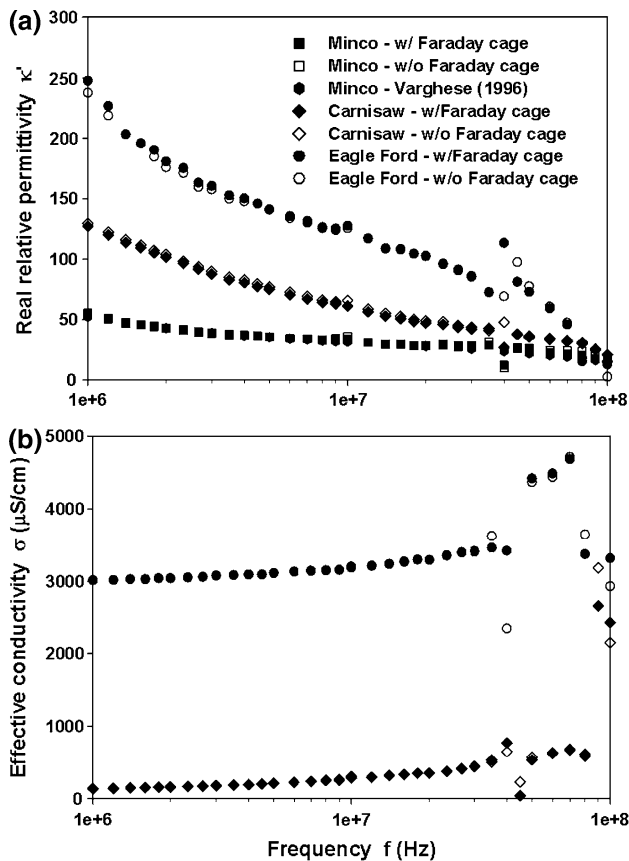


Fig. 3 Effect of Faraday cage on the dielectric measurements

ensure consistency and repeatability of the test results, the Faraday cage was used in all dielectric measurements.

4.2 Separate implementation of the two electrode pairs

As discussed briefly before, simultaneous implementation of the two pairs of electrodes is not recommended because electronic interactions increase the measurement of both real permittivity and effective conductivity. This phenomenon is highlighted in Fig. 4 for the results of a compacted Carnisaw sample.

Such an interaction affects the real permittivity when using the horizontal electrode pair (the one performing the horizontal measurement) more significantly than the vertical (the pair conducting the vertical measurement). This may be due to the relative geometric alignment of the two pairs when they are used in combination which promotes charge movement that strengthens interfacial polarization. The influence of electrode interaction on the measurement of effective conductivity influences each pair to a similar extent (Fig. 4). The existence of the second pair of electrodes shortens the peripheral electrical paths for the test electrodes providing overestimation of the electrical conductivity.

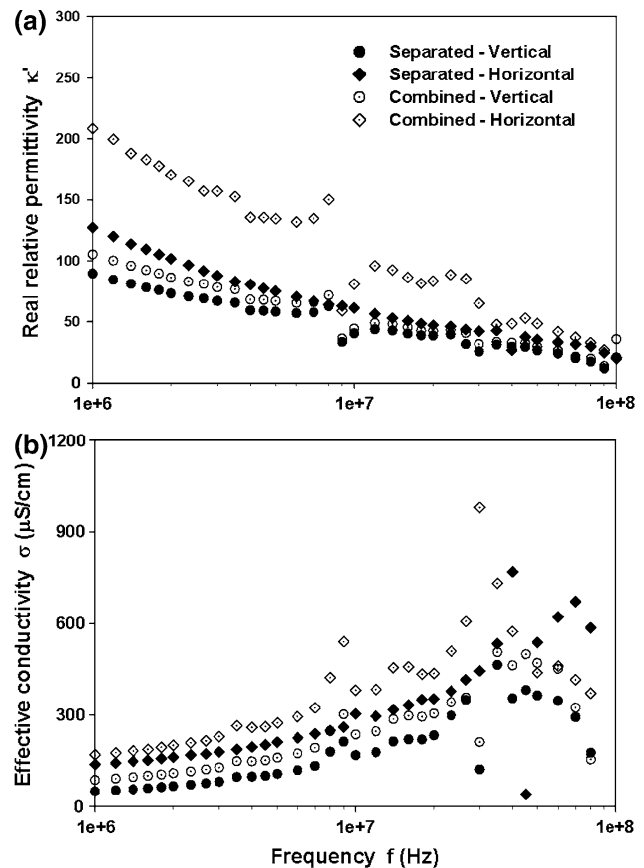


Fig. 4 Separated versus combined applications of the two pairs of electrodes

4.3 Measurement accuracy and repeatability

The major problem associated with the two-terminal electrode system in the radio frequency range is electrode polarization caused by charge accumulation on the surface of electrodes. This charge accumulation results in the formation of an electrical double layer that modifies the ion distribution within the sample under investigation. Electrode polarization has been revealed [7, 13, 14] based on testing various electrolyte solutions. For a specific soil–electrolyte mixture, however, the lower frequency boundary at which electrode polarization becomes negligible is still uncertain and can only be approximated [14]. The lower frequency boundary of the soils investigated in this study was estimated to vary within 50 kHz–2 MHz. Please note that the frequency boundary at which effective conductivity is affected by electrode polarization is much lower than that of real permittivity as discussed earlier in the literature review.

The measured real permittivity curves exhibit satisfactory continuity (Figs. 3, 4), whereas the effective conductivity measurement produces highly scattered data at frequencies greater than 20 MHz. This phenomenon may

be attributed to the limitations of the two-terminal system in measuring effective conductivity at the frequency range beyond 20 MHz. A network analyzer in conjunction with a coaxial probe test configuration was shown to provide continuous measurement of soil conductivity (from 20 MHz to 1.3 GHz)—see Klein [16]. The measurement of real permittivity using the two-terminal system, however, is highly repeatable as shown by the comparison of the data of this study versus those of Varghese [35] (Fig. 3). To further ensure repeatability using the two-terminal system, additional tests were conducted on Hollywood and Heiden soils providing corroboration of the real permittivity (1 MHz–100 MHz) and effective conductivity (1 MHz–20 MHz) data.

5 Quantification of diffuse double layer

It is necessary to quantify the diffuse double layer (DDL) and pore fluid conductivity that will be held responsible for a possible explanation of the dielectric responses of each soil presented later. However, the thickness of the DDL remains, in many respects, a theoretical concept [22]. The equation proposed by Mojid and Cho [22], described as the thickness of DDL equal to the “critical state water content” normalized by S_a and density of water, was constrained by the absence of dissolved solutes. It predicted DDL thicknesses for sand–bentonite mixtures in distilled water within a range of 5–107 % difference in comparison with the method of Schofield [28], but showed 507–9,834 % larger DDL thicknesses for mixtures with salt existence in the suspension [22]. The method of Mojid and Cho [22], therefore, was not considered in this study due to the possibility of salt presence in natural expansive soils.

Schofield [28] described the thickness of a fully developed DDL as

$$t_1 = \frac{q}{\sqrt{v\beta n}} - \frac{4}{v\beta\Gamma} \quad (6)$$

The DDL thickness can also be evaluated as the Debye–Hückel length [31] and expressed as

$$t_2 = \sqrt{\frac{\varepsilon_0 R \kappa' T}{2 F^2 n v^2}} \quad (7)$$

Within Eqs. (6) and (7), q is a factor dependent on cation versus anion ratio (e.g., 2 for NaCl and 1.46 for Na_2SO_4), v is cation valence, β stands for $8\pi F^2/(\varepsilon_0 \kappa' RT)$, $\varepsilon_0 = 8.85 \times 10^{-12}$ F/m is permittivity of vacuum, κ' is defined in Eq. (2), $F = 9.6485 \times 10^4$ C/mol is Faraday constant, $R = 8.314$ J/(K mol) is gas constant, T is absolute temperature ($=298.15$ K here), n is salt concentration (mol/m^3), Γ is surface charge density (meq/m^2).

In order to deduce salt concentration, n , a convenient and universal approach is to create 1:5 soil water mixtures from which the dc conductivity of the bulk fluid (extracted liquid after filtering), σ_{bl_1} , is obtained [23, 25]. It is worth mentioning that “bulk fluid” refers to the fluid phase of a soil suspension, while “pore fluid” represents the fluid phase of a compacted or consolidated soil sample. The magnitude of σ_{bl_1} was measured in this study using a calibrated conductivity benchtop manufactured by Thermo electron corp. A value of 1 mS/cm approximately equals 640 mg/L of soluble salts [23, 29]. Additional sulfate tests following OHD L-49 [24] were carried out, and sulfate was only detected in Eagle Ford with a recorded value of 354 ppm. Provided SO_4^{2-} and Cl^- are the most frequently existing anions in soil salts [25]; for simplicity purposes, Na_2SO_4 was assumed as the salt in the extracted liquid of Eagle Ford, and NaCl was assumed for the other three soils; therefore, the salt concentration, n , can be transformed from mass per volume to molarity per volume. The bulk fluid (extracted liquid) was then measured for κ'_{bl} and σ_{bl_2} using the dielectric measurement setup shown in Fig. 1. For electrolytes only (without soil inclusion), effective conductivity does not vary with frequency (within radio frequency range) and is approximately equal to the dc conductivity. The estimated parameters used to calculate the DDL thicknesses using two theories (t_1 and t_2) are listed in Table 4. The magnitudes of σ_{bl_1} measured using a dc conductivity probe, and σ_{bl_2} of the extracted liquid measured in the dielectric setup, are relatively close. The favorable comparison between σ_{bl_1} and σ_{bl_2} further verifies the dielectric measurement methods of this study. The dielectric measurements were conducted on the bulk fluid not only for such a verification purpose but also to obtain the value of κ'_{bl} , which is used to calculate the DDL thickness.

The fully developed DDL thickness in each soil, t_1 and t_2 , as calculated from Eqs. (6) and (7), respectively, compares well. In both equations, the DDL thickness is largely governed by the bulk fluid concentration, n , which is revealed by the bulk fluid conductivity regardless of the physicochemical nature of the clay particle itself. The n governs the DDL thickness calculations in part because κ' of an electrolyte remains nearly constant with varying salt concentrations [7]. In addition, assumption of other salt types has little impact on the thickness and will not change the sequence (Carnisaw > Hollywood > Heiden > Eagle Ford), rendering the bulk fluid conductivity (σ_{bl_1} or σ_{bl_2}) the determining factor in evaluating DDL thickness. Therefore, it is not surprising that Carnisaw shows a significantly thicker DDL than that of the much more plastic Eagle Ford concerning the markedly greater conductivity of the extracted liquid of Eagle Ford. It must be noted that

Table 4 Estimated thickness of fully developed DDL

Soil sample	$\sigma_{bl,1}$ ($\mu\text{S}/\text{cm}$)	$\sigma_{bl,2}^a$ ($\mu\text{S}/\text{cm}$)	κ_{bl}^a	n (mol/m^3)	Γ^b (meq/m^2)	t_1 (μm)	t_2 (μm)	Variation ^c (%)
Carnisaw	21	23	86	0.23	2.54×10^{-3}	0.012	0.021	44
Hollywood	105	105	83	1.15	1.81×10^{-3}	0.005	0.009	44
Heiden	149	156	87	1.63	2.21×10^{-3}	0.004	0.008	44
Eagle Ford	1,344	1,292	84	6.06	2.32×10^{-3}	0.002	0.004	59

^a Do not vary with frequency for electrolytes within the radio frequency range

^b $\Gamma \approx \text{CEC}/S_a$ [31]

^c Variation = $(t_2 - t_1)/t_2$

even though there is a parameter Γ (controlled by S_a and CEC) on the right side of Eq. (6), the magnitude of the second term is much smaller than the first and can be ignored [22].

The thickness data (t_1 and t_2) deduced in Table 4 are representative of the fully developed state of the DDL when the clay particles are hydrated in 1:5 soil water suspensions. The electromagnetic properties of the pore fluid phase of a compacted or consolidated oedometer soil sample are not currently measurable, and thus the corresponding DDL thickness cannot be quantified. Instead, the DDL thickness can be qualitatively analyzed for an oedometer soil sample because its soil–water ratio is much higher than when in suspension, which means a relative increase in concentration, n . The interaction of adjacent particles is enhanced, resulting in DDL contraction. Furthermore, the development of DDL is suppressed as the sample becomes unsaturated. On the other hand, the bulk fluid conductivity (measured on extracted liquid of a soil suspension) is used to qualitatively represent the pore fluid conductivity (conductivity of the pore fluid phase of an oedometer soil sample) because the latter is not, at present, experimentally achievable (the dielectric measurements on an oedometer soil sample obtain effective conductivity of the entire sample).

Another quantitative description of DDL is surface conductance λ_{ddl} (Table 2), which when normalized by the DDL thickness produces surface conductivity (conductivity of the DDL) [31], σ_{ddl} . The degree of interfacial polarization of clayey soils is determined by the difference in magnitude between surface conductivity σ_{ddl} and that of pore fluid σ_{el} [19, 31]. Since σ_{el} (also a constant) is not directly measurable, its magnitude was qualitatively evaluated by σ_{bl} instead. The comparison of σ_{ddl} with the bulk fluid (electrolyte) conductivity, σ_{bl} , is illustrated in Table 5.

Table 5 shows that if the contribution of hydrogen to λ_{ddl} is not accounted for then the sequence of the magnitude of $(\sigma_{ddl}-\sigma_{bl})$ accurately corresponds with the ranking of the extent of interfacial polarization phenomenon indicated in Fig. 5. The smaller magnitude of $(\sigma_{ddl}-\sigma_{bl})$ of

Carnisaw is more reasonable, owing to the fact that the hydrogen ion diffuses much more rapidly than the other types of cations in the free liquid phase so that the associated conductivity may not contribute to the conduction of the diffuse ion swarm constrained around clay surfaces. Another profound feature of Table 5 is the overwhelming magnitude of σ_{ddl} relative to that of σ_{bl} . This may arise from the underestimation of diffuse double layer thickness (t_{avg}) due to its predominant dependence on bulk fluid concentration (as discussed earlier) that leads to over-prediction of σ_{ddl} ; on the other hand, the usage of σ_{bl} instead of σ_{el} may result in underestimated conductivity of the pore fluid phase in a soil sample.

6 Electromagnetic test results and discussion

6.1 Dielectric responses with frequency

The dielectric test method introduces a convenient approach to study the electromagnetic behavior of soil samples that are suitable for conventional oedometer testing. Even though the dielectric measurements were performed in the device frequency range of 400 kHz–110 MHz, the permittivity, κ' , and conductivity, σ , data were presented for the frequency range of 1 MHz–100 MHz only, within which the effects of electrode polarization were minimized and electronic resonance (at 110 MHz) avoided. The dielectric spectra of the four studied samples are presented in Fig. 5.

Both κ' , σ and the dispersion of κ' increase in magnitude in the order of Carnisaw < Hollywood < Heiden < Eagle Ford. This sequence coincides with the order of the magnitude difference of $(\sigma_{ddl}-\sigma_{bl})$ (Table 5), which determines the degree of interfacial polarization, regardless of the measurement direction. Surface conduction (the act of surface conductance λ_{ddl}) has been shown as the dominant mechanism in determining the polarization and conduction and an important contributor to global soil conductivity in pure clay saturated with low ionic concentration pore fluid [15, 31]. It is therefore proven here that the degree of

Table 5 Surface conductivity versus bulk fluid conductivity and the magnitude of difference

Soil sample	λ_{ddl} (μS)	t_{avg}^a (μm)	σ_{ddl} ($\mu\text{S}/\text{cm}$)	σ_{bl}^b ($\mu\text{S}/\text{cm}$)	$\sigma_{ddl}-\sigma_{bl}$ ($\mu\text{S}/\text{cm}$)
Carnisaw ^c	0.080 ^c	0.016	48,597 ^c	24	48,574 ^c
Carnisaw ^d	0.002 ^d	0.016	1,032 ^d	24	1,008 ^d
Hollywood	0.011	0.007	15,024	105	14,918
Heiden	0.013	0.006	20,957	156	20,801
Eagle Ford	0.014	0.003	47,659	1,292	46,367

^a Average of t_1 and t_2 given in Table 4

^b The values of $\sigma_{bl,2}$ (Table 4) are used

^c Taking into account the contribution of hydrogen

^d Excluding the effect of hydrogen

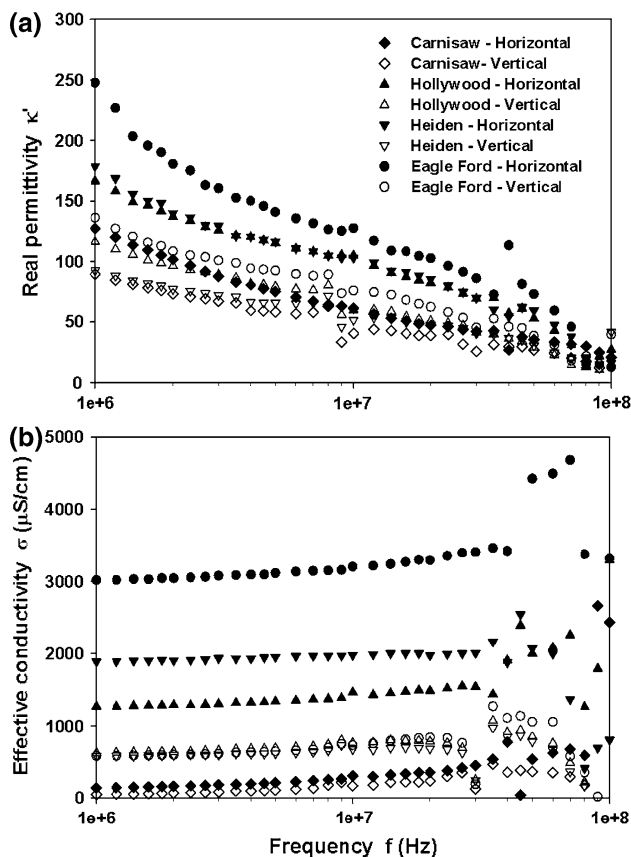


Fig. 5 Real permittivity and effective conductivity curves of the studied samples

interfacial polarization across the radio wave frequency range can be qualitatively predicted by the quantities of $(\sigma_{ddl}-\sigma_{bl})$. Meanwhile, a comparison of Table 4 and Fig. 5 indicates that both the bulk fluid conductivity σ_{bl} and the conductivity of the compacted sample, σ , follow the same order of Carnisaw < Hollywood < Heiden < Eagle Ford. This suggests that the pore fluid conduction can contribute substantially to the effective conductivity of a compacted natural expansive soil. It must be noted that surface conduction plays the predominant role in determining the

overall conductivity of clay suspension washed with de-ionized water (the reason why the clay–water mixture conductivity is greater than that of water). As the bulk fluid concentration increases, the bulk fluid conductivity, σ_{bl} , begins to take on a more important role in controlling the suspension conductivity [19, 27]. Nevertheless, the contribution of pore fluid conductivity, σ_{el} , relative to surface conductivity, σ_{ddl} , of a compacted or consolidated sample is not well understood yet due to the fact that the pore fluid conductivity, σ_{el} , of a compacted or consolidated sample is not experimentally achievable. At the same time, all of the samples exhibit various degrees of electrical anisotropy as implied by the higher measurement of κ' and σ in the horizontal, rather than the vertical direction.

6.2 Evaluation of anisotropy based on κ'_{inf} and σ_{dc}

The electromagnetic properties of a compacted or consolidated sample are dependent on water content, mineralogy, microstructure and σ_{dc} of the liquid phase (pore fluid). Interfacial polarization functions as the major polarization mechanism occurring within the radio frequency range; however, the κ' becomes nearly constant and independent of frequency when the frequency reaches a certain value where there is not enough time for charge accumulation at the interfaces [1]. The κ' at this point, which was defined as κ'_{inf} [1, 31], is also independent of pore fluid conductivity, σ_{el} , which only affects the electromagnetic properties during relaxation. In short, for a specific soil (with fixed mineralogy), κ'_{inf} reveals the intrinsic particle/aggregate shape and alignment and the state of saturation in macro and micro pores. In the works of several researchers [2, 4, 9, 12, 35], κ'_{inf} was taken to be the magnitude of permittivity at 50 MHz and shown to be mainly a function of saturation ratio, microstructure and mineralogy while independent of pore fluid chemistry. The analysis of real permittivity dispersion, however, is complicated by the ionic conductivity of the pore fluid (σ_{el}). Moreover, the magnitude of dispersion may suffer from electrode polarization at low MHz

frequencies as discussed earlier, the effect of which can hardly be quantified. In this regard, this study qualitatively evaluated the dielectric dispersion behavior and quantitatively analyzed the κ'_{inf} magnitude during various stages of deformation.

The effective conductivity, σ , is a product of the interaction between DDL and pore fluid and varies with frequency. The σ below 1 MHz has been used to evaluate soil anisotropy [15, 21] and estimate stiffness and liquefaction of granular soils [3, 5]. As has been illustrated (Figs. 4, 5), the measurement of σ with the test system in this study is satisfactory up to 20 MHz, while electrode polarization has little influence on the conductivity measurement at the frequency range concerned (1 MHz–100 MHz). Moreover, since the contribution of the polarization loss to σ becomes trivial at frequencies less than 1 MHz, the σ value at these frequencies can be used to approximate the dc conductivity of a soil–electrolyte mixture [18, 19], marked here by σ_{dc} . As a result, for the oedometer soil samples concerned, σ at 1 MHz is taken as the approximate magnitude of σ_{dc} . It must be noted that this σ_{dc} represents the dc conductivity of the entire soil sample, which combines the effects of both pore fluid conduction and surface conduction.

In this context, the electrical anisotropy of the samples at the compacted state can be evaluated as the ratio of κ'_{inf} and σ_{dc} measured at two directions, as illustrated in Table 6.

For the samples investigated, the tendency for the platy clay particle or elongated aggregates to have their long axis oriented in the horizontal plane favors the contribution of surface conduction to the sample conductivity when exposed to the horizontal electrical field, while the tortuosity of pore fluid path is substantially decreased in the horizontal direction. The larger $(\kappa'_{\text{inf}})_{\text{h}}$ than $(\kappa'_{\text{inf}})_{\text{v}}$ implies that the strengthened effect of surface conduction overcompensates for the enhanced contribution from pore fluid conduction, whereas such an alignment strengthens the contributions of both pore fluid conduction and surface conduction to the overall $(\sigma_{\text{dc}})_{\text{h}}$ relative to $(\sigma_{\text{dc}})_{\text{v}}$. Therefore, the electrical anisotropy acts as a direct reflection of structural anisotropy. Such anisotropy is revealed more substantially in the case of Eagle Ford (Table 6), regarding

Table 6 Evaluation of sample anisotropy based on κ'_{inf} and σ_{dc}

Soil sample	$(\kappa'_{\text{inf}})_{\text{h}}$	$(\kappa'_{\text{inf}})_{\text{v}}$	$(\sigma_{\text{dc}})_{\text{h}}$	$(\sigma_{\text{dc}})_{\text{v}}$	$(\kappa'_{\text{inf}})_{\text{h}}/(\kappa'_{\text{inf}})_{\text{v}}$	$(\sigma_{\text{dc}})_{\text{h}}/(\sigma_{\text{dc}})_{\text{v}}$
Carnisaw	35.6	26.8	138	49	1.33	2.82
Hollywood	52.8	29.0	1269	621	1.82	2.04
Heiden	59.4	30.4	1888	576	1.96	3.28
Eagle Ford	73.1	38.6	3018	578	1.89	5.22

Subscripts “h” and “v” represent the horizontal and vertical directions, respectively

its greater S_{a} and larger, thinner clay platelets in a more laminar microstructure when compared to the case of Carnisaw (Fig. 6).

6.3 Evolution of κ'_{inf} and σ_{dc} with deformation

Each compacted sample followed a procedure of free expansion–compression–rebounding–recompression using the setup shown in Fig. 2. The relationships of κ'_{inf} and σ_{dc} (obtained from vertical measurements) with deformation are plotted in Fig. 7. The horizontal measurement of κ'_{inf} and σ_{dc} was not possible at this stage due to the limitation of the setups (separate use of the electrode pairs).

Both κ'_{inf} and σ_{dc} increase monotonically with the vertical expansion during the first stage of deformation (free swelling). Beyond this stage, the magnitudes become relatively insensitive to soil deformation. This phenomenon implies that the parameters κ'_{inf} and σ_{dc} of a single soil sample are primarily dependent on the saturation ratio, since the free swelling also acts as a hydration process, whereas the following stages are merely compression–rebounding–recompression of saturated samples. The hydration process interconnects previously isolated clay aggregates by gradually filling macropores, resulting in well-developed continuous flow paths favoring electrical conduction. Further widening or collapsing of macropores during the following deformation stages only slightly affect the pore fluid conduction. This also implies that the increase of σ_{dc} throughout the swelling process resulted mostly from the increase in continuous electrically conductive pathways in the pore fluid phase.

6.4 Discussion of the roles of DDL and σ_{dc} on dielectric responses

Provided the much greater PI (Table 1) and higher montmorillonite content (Table 3) of Eagle Ford than those parameters of Carnisaw, a thicker DDL (when fully developed) of Eagle Ford tends to be expected. However, both the conduction and thickness of DDL in the case of Carnisaw turned out to be higher. In this regard, it may be necessary to re-evaluate the current Gouy–Chapman theory to take into account the impact of soil mineralogy and microstructure.

For clay–water mixtures where the pore fluid concentration is relatively low (e.g., up to the level in this study), surface conduction plays the major role in controlling the extent of interfacial polarization and the effective conductivity of the mixture, revealed as enhanced dielectric dispersion, real permittivity and effective conductivity of a clay–water mixture relative to the electrolyte only. Meanwhile, the contribution of surface conduction is revealed to

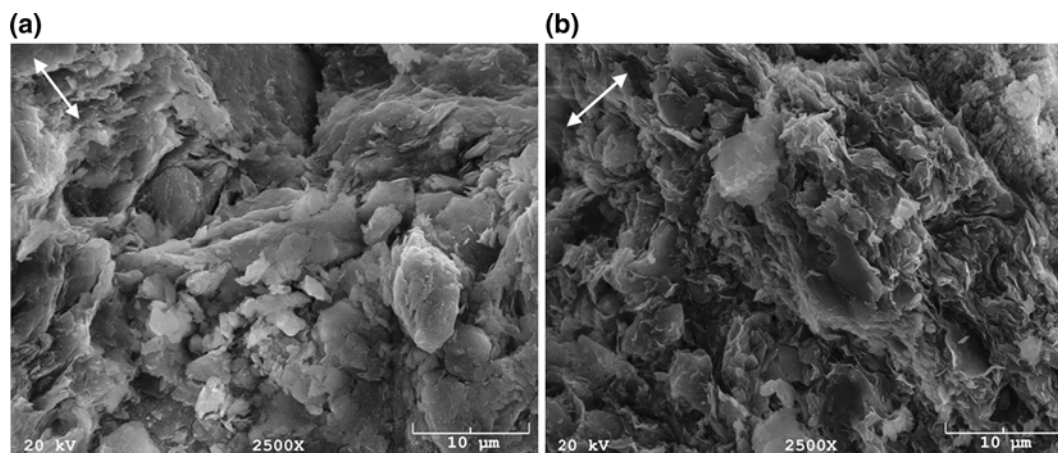


Fig. 6 SEM micrographs of **a** Carnisaw and **b** Eagle Ford (Arrows marking the direction of compaction)

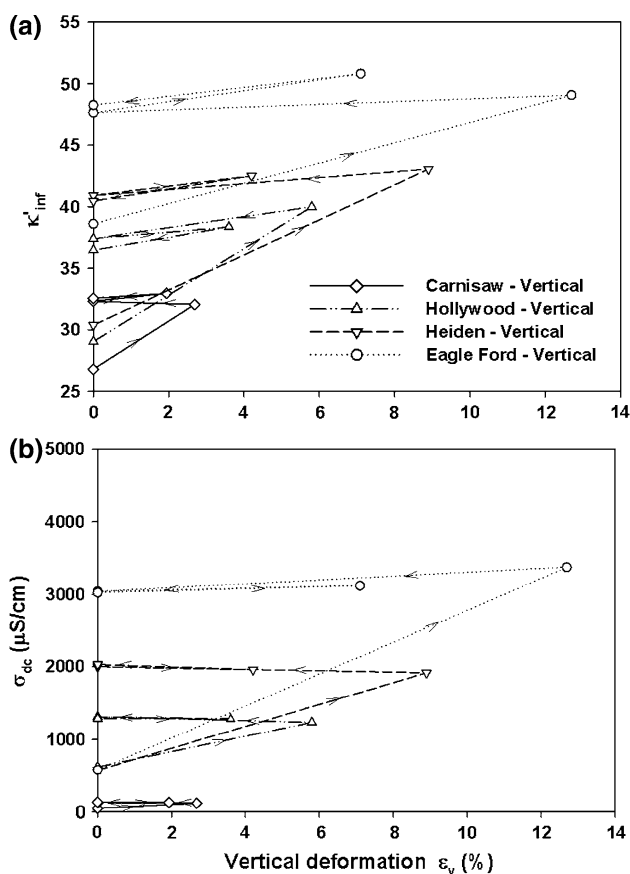


Fig. 7 κ'_{inf} and σ_{dc} versus deformation of the studied samples

be affected by mineralogy, pore fluid chemistry, microstructure and water content. On the other hand, the development of pore fluid conduction is influenced by microstructure and water content as indicated by the anisotropy (Fig. 5; Table 6) and the increase of σ_{dc} with the hydration process (Fig. 6). Nevertheless, the magnitude of pore fluid conductivity, σ_{el} , is not yet measurable in a

soil sample under hydromechanical conditions and therefore may only be evaluated from the bulk fluid (liquid extract) conductivity, σ_{bl} , of a soil.

7 Final comments and conclusions

In this study, the real permittivity and effective conductivity of four natural expansive soils were obtained from dielectric measurements using a two-terminal electrode system and a modified oedometer cell. Several comments and conclusions follow.

1. A special dielectric test procedure was developed by adopting the method of a two-terminal electrode system. This test can measure the initial electromagnetic properties of an undisturbed or compacted soil sample in directions normal to or parallel with that of consolidation/compaction, with the use of different pre-calibrated test setups. Moreover, integration of dielectric measurements with a modified oedometer cell accommodates the monitoring of dielectric responses of soil samples under various hydromechanical conditions.
2. Efforts were directed toward quantification of DDL (in its fully developed state) in terms of thickness and surface conductance/conductivity. Two approaches in estimating the DDL thickness achieved close results with a variation less than 59 %. The thickness was largely influenced by the salt concentration, n , in the bulk fluid of the studied soil samples implied by its decrease with increasing concentration, regardless of soil type. However, neither mineralogy nor microstructure was accounted for in the underlying theory.

The development of DDL in a soil sample is restrained by the interaction from adjacent particles as well as intrusion of air if the sample becomes unsaturated.

- Interfacial polarization serves as the predominant polarization mechanism in the radio frequency range of 1 MHz–100 MHz not only for pure clay–water mixtures but also for naturally collected expansive soils. The measure of the polarization is well evaluated by the difference between the surface conductivity σ_{ddl} and the pore fluid conductivity σ_{el} but was quantified as $(\sigma_{ddl} - \sigma_{bi})$ because of the challenge in obtaining σ_{el} . Electrical anisotropy was seen with higher real permittivity and effective conductivity measurements in the horizontal rather than the vertical direction, as a result of structural anisotropy and can be quantified by $(\kappa'_{inf})_h / (\kappa'_{inf})_v$ or $(\sigma_{dc})_h / (\sigma_{dc})_v$. Meanwhile, the electrical anisotropy was more significant for samples with larger surface area (S_a).

Based on the experimental information provided by this study, the investigation of κ'_{inf} and σ_{dc} introduced a way to assess the hydraulic state and structural anisotropy of expansive soils. Further research is aimed at determining a quantitative relationship of κ'_{inf} and σ_{dc} with matric suction for individual expansive soils through the integration of a suction-controlled system. Combined assessments of geophysical and mechanical models are necessary for prospective physical modeling of hydromechanical behavior of clayey soils. Improvement on quantifying DDL thickness and conductivity, measurement of pore fluid conductivity and evaluation of the role of surface conductivity relative to pore fluid conductivity in contribution to effective conductivity of a consolidated/compacted sample will also be topics of interest.

Acknowledgments Financial support for this research was provided by the National Science Foundation (Grant No. 0746980). The support is greatly appreciated. The authors also owe gratitude to Prof. Kanthasamy K. Muraleetharan, Prof. James K. Mitchell and Prof. Federico Bordi for their valuable guidance and comments.

References

- Arulanandan K (2003) Soil structure: in situ properties and behavior. Soil structure: in situ properties and behavior, Davis
- Arulanandan K (1991) Dielectric method for the prediction of porosity of saturated soils. *J Geotech Eng* 117(2):319–330
- Arulanandan K, Muraleetharan KK (1988) Level ground soil-liquefaction analysis using in situ properties. *J Geotech Eng Div ASCE* 114(7):771–790
- Arulanandan K, Yogachandran C (2000) Dielectric method for non-destructive characterization of soil composition. GeoDenver 2000, ASCE Geo-Institute, ASCE special publication
- Arulmoli K, Arulanandan K, Seed HB (1985) New method for evaluating liquefaction potential. *J Geotech Eng Div ASCE* 111(1):85–114
- ASTM (2011) 2011 Annual Book of ASTM Standards. Volume 04.08 Soil and Rock (I): D420–D5876 and Volume 4.09 Soil and Rock (II): D5877—latest. West Conshohocken, Pennsylvania
- Bordi F, Camitti C, Gili T (2001) Reduction of the contribution of electrode polarization effects in the radiowave dielectric measurements of highly conductive biological cell suspensions. *Bioelectrochemistry* 54:53–61
- Bredenkamp S, Lytton RL (1994) Reduction of sulfate swell in expansive clay subgrades in the Dallas district. Texas Transportation Institute, Research Report 1994–5, p 124
- Campbell JE (1990) Dielectric properties and influence of conductivity in soils at one to fifty megahertz. *Soil Sci Soc Am J* 54:332–341
- Cerato AB, Lin B (2012) Dielectric measurement of soil-electrolyte mixtures in a modified oedometer cell using 400 kHz to 20 MHz electromagnetic waves. *ASTM Geotech Test J* 35(2):1–9
- Cerato AB, Lutenegger AJ (2002) Determination of surface area of fine-grained soils by the ethylene (EGME) method. *ASTM Geotech Test J* 25(3):315–321
- Fernando MJ, Burau RG, Arulanandan K (1977) A new approach to determination of cation exchange capacity. *Soil Sci Soc Am J* 41(4):818–820
- Klein K, Santamarina JC (1996) Polarization and conduction of clay-water-electrolyte systems. *J Geotech Eng Nov.*:954–955
- Klein K, Santamarina JC (1997) Methods for broad-band dielectric permittivity measurements (soil–water mixtures, 5 Hz to 1.3 GHz. *ASTM Geotech Test J* 20(2):168–178
- Klein K, Santamarina JC (2003) Electrical conductivity in soils: underlying phenomena. *J Environ Eng Geoph* 8(4):263–273
- Klein K (2004) Permittivity measurements of high conductivity specimens using an open-ended coaxial probe—measurement limitations. *J Environ Eng Geoph* 9(4):191–200
- Lin B, Cerato AB (2012) Prediction of expansive soil swelling based on four micro-scale properties. *B Eng Geol Environ* 71:71–78
- Liu N, Mitchell JK (2009) Modeling electromagnetic properties of saturated sand and clay. *Geomech Geoeng* 4(4):253–269
- Liu N, Mitchell JK (2009) Effects of structural and compositional factors on soil electromagnetic properties. *Geomech Geoeng* 4(4):271–285
- Lyklema J (1995) Fundamentals of interface and colloid science volume II: solid–liquid interfaces. Academic press, New York
- Meegoda NJ, King IP, Arulanandan K (1989) An expression for the permeability of anisotropic granular media. *Int J Numer Anal Methods Geomech* 13(6):575–598
- Mojid MA, Cho H (2006) Estimating the fully developed diffuse double layer thickness from the bulk electrical conductivity in clay. *App Clay Sci* 33:278–286
- Munns R (2004) Salinity stress and its impact. Plant Stress Website. In: Blum A (ed). <http://www.plantstress.com/Articles/index.asp>
- OHD L-49 (2005) Method of test for determining soluble sulfate content in soil. Oklahoma Department of Transportation, Oklahoma
- Pansu M, Gautheyrou J (2006) Chapter 18: “soluble salts”, handbook of soil analysis-mineralogical, organic and inorganic methods. Springer, p 1012
- Parkhomenko EI (1967) Electrical properties of rocks. Plenum Press, New York 314
- Raythatha R, Sen PN (1986) Dielectric properties of clay suspensions in MHz to GHz range. *J Colloid Interf Sci* 109(2): 301–309

28. Schofield RK (1947) Calculation of surface areas from measurements of negative adsorption. *Nature (London)* 160:408–410
29. Silva JA, Uchida R (2000) Plant nutrient management in Hawaii's soils, approaches for tropical and subtropical agriculture. University of Hawaii at Manoa, p 158
30. Rhoades JD (1982) Cation exchange capacity. In: Page AL et al (ed) *Methods of soil analysis*. Agronomy 9, 2nd edn. American Society of Agronomy, Madison, pp 159–165
31. Santamarina JC, Klein K, Fam M (2001) *Soils and waves: particle materials behavior, characterization and process monitoring*. Wiley, Chichester, p 488
32. Selig ET, Mansukhani S (1975) Relationship of soil moisture to the dielectric property. *Geotech Eng Div Eng Div Am Soc Civil Eng Proc* 101(GT8):755
33. Thevanayagam S (1993) Electrical response of two-phase soil: theory and applications. *J Geotech Eng* 119(8):1250–1275
34. USGS Open-File Report (2001) A laboratory manual for X-ray-powder diffraction. <http://pubs.usgs.gov/of/2001/of01-041/>
35. Varghese S (1996) Use of electrical measurements to determine soil properties and identify the presence of contaminants in soils. A project report for the school of Civil Engineering and Environmental Sciences, the University of Oklahoma, p 48